Ball Drop Simulation on Two-Way Radio Lens Using ABAQUS/Explicit

Ben Nagaraj, Doug Carroll, and Ted Diehl
Motorola, Plantation
8000 W. Sunrise Blvd.
Fort Lauderdale, FL 33322

Abstract

Explicit dynamic simulations are increasingly being used by commercial industry to analyze structures enduring drop and impact loading. To demonstrate the application of this technology, a detailed study of modeling techniques required to compute ball drop simulations on a two-way radio lens is performed. The study looks at issues ranging from the transformation of CAD geometry into usable explicit dynamic models to detailed modeling approaches used for analyzing contact and highly nonlinear elastic material behavior. The evaluation concludes by analyzing a detailed model consisting of 16 different parts that are predominately constrained together with 13 separate contact pairs. The paper discusses the modeling methodology utilized, its success, and some of the challenges faced in simulating this type of elastically-dominated impact problem.

1.0 Introduction

Hand-held communication devices such as two-way radios and cellular phones increasingly rely on larger displays to enhance functionality. Due to the fragile nature of glass and displays in general, designs must ensure that these components are robust against accidental shock induced by dropping the radio or directly impacting the display. This paper discusses using ABAQUS/Explicit to analyze the impact behavior of a two-way radio display. The methodology and issues involved are demonstrated via a ball-drop impact simulation consisting of dropping a 32 mm diameter steel ball from a height of 0.5 m directly onto the display lens of the radio.

A typical two-way radio is displayed in Figure 1. From a structural viewpoint, the radio consists of front and back plastic housings, a display assembly, and a main PCB (printed circuit board) assembly. The front housing contains a clear plastic lens that protects the display assembly. Generally, a display assembly consists of a glass LCD, plastic lightpipe, display driver PCB, plastic spacer, and elastomeric pads (cushions). All of these display components are stacked together, constrained predominately by contact, and mounted between the inside surface of the front housing and the main board. As shown, the main board has numerous components soldered onto it: integrated circuits, discrete components, and shields (typically 5-sided sheet metal boxes). The entire radio is then constrained together with a few screws, adhesives, and mating features such as grooves, channels, snaps, and connectors.

From a modeling viewpoint, especially relative to a drop or impact analysis, much of the radio is held together (or interacts) via contact constraints. The most practical method to model the

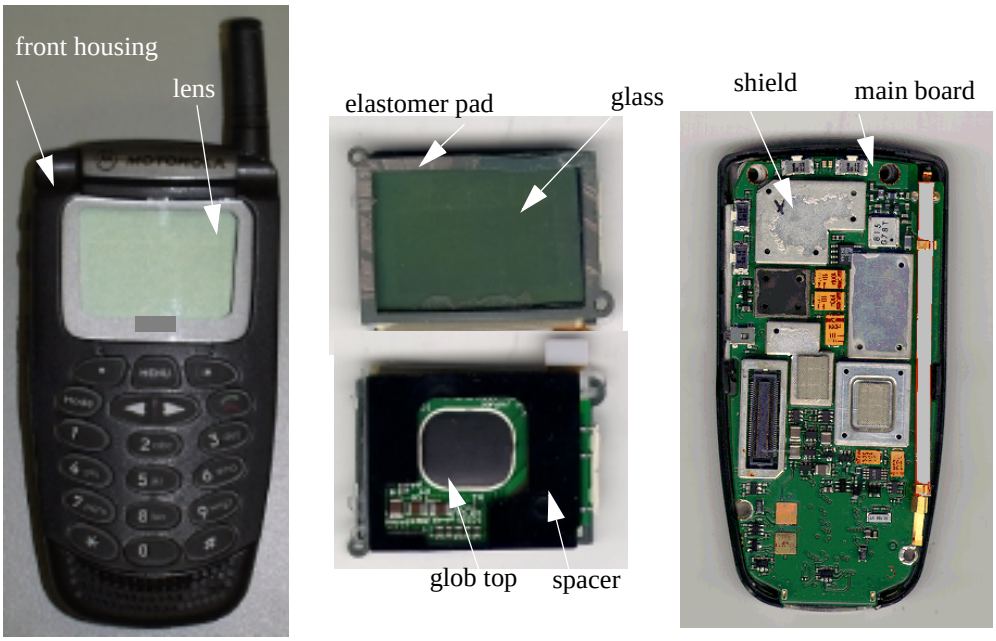

Figure 1: Typical two-way radio

impact behavior of such a complex structure is via explicit dynamics. Some of the issues that must be addressed for these impact models are: (i) transformation of complex CAD geometry into suitable FE meshes, (ii) modeling of components using shell elements, (ii) modeling of thin elastomeric foam pads (cushions), and (iv) constraining numerous parts via contact.

2.0 Systemic Modeling Issues

The first step in FE modeling is to simplify the CAD geometry by removing non-structural components and features that are not relevant to structural integrity. Possibly the most time consuming problem that must be addressed is the transformation of the simplified CAD geometry to FE meshes. Meshing tools inside CAD programs (such as Pro/E) are still too limited to completely deal with the meshing of complex models that utilize a combination of solids, shells, and numerous contact conditions. Additionally, importing complex CAD solid geometry into FE preprocessors (such as PATRAN) does not always work. Thus, a combination of methods must be used to create FE models in timely manner. This hybrid approach consists of (i) meshing some of the components in the CAD tool, (ii) importing some CAD components and/or subassemblies directly and via IGES into a FE preprocessor for meshing, and (iii) defining contact pairs in the preprocessor and/or directly in the FE input file (via manual editing).

It is common practice to utilize shell elements for modeling thin structural components. This causes several challenges, especially when several shell components must interact via contact

constraints. Transforming and modeling solid CAD geometry into shell elements is still not a turnkey operation. CAD and preprocessor tools fail quite frequently when attempting to generate mid-plane surfaces (or meshes) of structures with numerous internal features such as ribs, stiffeners, tabs, and locating indents. ABAQUS' new OFFSET feature under the *SHELL SECTION command helps minimize this problem by allowing the analyst to place a shell mesh on any coinvent surface of the to-be-shelled solid. The OFFSET parameter is then used to specify the offset of the mesh's "nodal plane" from the true mid-plane of the structure. Another difficulty with shells is the modeling of thin structures whose thickness varies continuously over the part, something that is now commonplace with product designs driven by industrial design sculpting. While ABAQUS offers a feature to include variations in shell thickness via a tabular definition of thickness at each node, there is no easy method to obtain such data from the solid CAD geometry. Lacking this method, the component is typically divided into several groups and average representative values of thickness are assigned to each of the groups. In many cases this can lead to notable stiffness inaccuracies as well as improper representations of contact surface location. Lastly, there are few tools, if any, that enable the analyst to visualize the shell elements as solids (including their OFFSETs). Without this type of feature, it is extremely difficult to debug and assess complex shell models that utilize numerous contact pairs.

Once solutions to the above issues are made readily available in FE modeling and analysis software, modeling time will be reduced drastically, accuracy of analyses can be improved, and more of this type of analysis can begin to move outside the domain of the "analyst." Hopefully, HKS' new ABAQUS/CAE product will be addressing all of these systemic issues as it develops in the future.

3.0 Preliminary Study

Figure 2 depicts a coarse model of a highly simplified two-way radio's display region. The model was used to study various modeling techniques and consisted of 12 meshed components and 2 analytical rigid surfaces. Figure 3 provides more detail of the 12 meshed components. Shell elements (S4R) were used for all components except the display lens and elastomeric pads which were modeled using solid elements (C3D8R). To mimic the difficulty of obtaining mid-plane surfaces, shell elements were generated at the top or bottom surface of various components. The new OFFSET feature in ABAQUS was used to correct for the actual location of the mid-plane. This correction not only makes prediction of the structure's stiffness more accurate, but more importantly, it allows contact surfaces to be represented more accurately. Components that were physically glued together were modeled using the TIED option on the *CONTACT PAIR definition. Using "tied contact" can significantly simplify model building since it removes the traditional requirement that components have common nodal locations at common boundaries. Linear elastic and elastic/plastic material models were used for all the components except the elastomeric foam pads, which were modeled with a one-term *HYPERFOAM model. The entire radio was then placed on top of a flat rigid surface (not shown, located under the back housing). The steel ball used to induce the impact was modeled using an analytical rigid surface and lumped

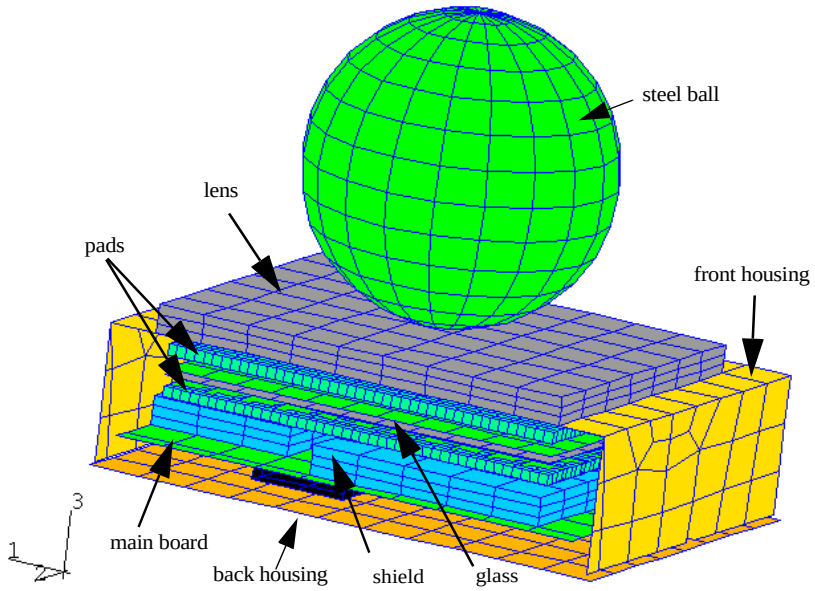

Figure 2: Coarse finite element model of a simplified two-way radio

mass element. The reference node of the steel ball was given an initial velocity of 3.13 m/sec (impact velocity for 0.5 m drop) and the model was defined to simulate 4 msec of physical time.

As is common with most non-trivial FEA models, debugging must be performed before the model will properly run. In this particular model, several unexpected problems occurred that needed to be resolved. Initial attempts to run the model failed with the code crashing in the datacheck phase - providing no error messages and no restart file. This made debugging extremely difficult. Eventually it was determined that severe contact overclosures in the initial configuration were causing the code to crash. These overclosures were caused by a “bull-nose” effect at the free-edge of the shell elements in the front housing which were contacting against the back housing. This “bull-nose” effect is caused by ABAQUS’ contact algorithm internally extending (artificially) all free-edges of contact surfaces with a radius equal to half the thickness of the surface (see Fig. 4). In this case, the overclosure problem was solved by decreasing the shell element boundary (at the edge) by half its thickness.

The analysis then ran for a few increments and halted due to severe overclosures. After some deductive reasoning, it was determined that the modeling of contact between a stack of three shells (each defined using the OFFSET option) caused the problem. Based on the data and overclosures reported, it appeared as though ABAQUS correctly found no overclosures initially, but as the analysis continued, it forgot about the OFFSET and started checking for contact closure as if the nodes were defined at the mid-surface of the shell element. This bug was reported and HKS states it has been fixed in V5.8. This problem was resolved (in V5.7) by moving one of the shell’s nodal

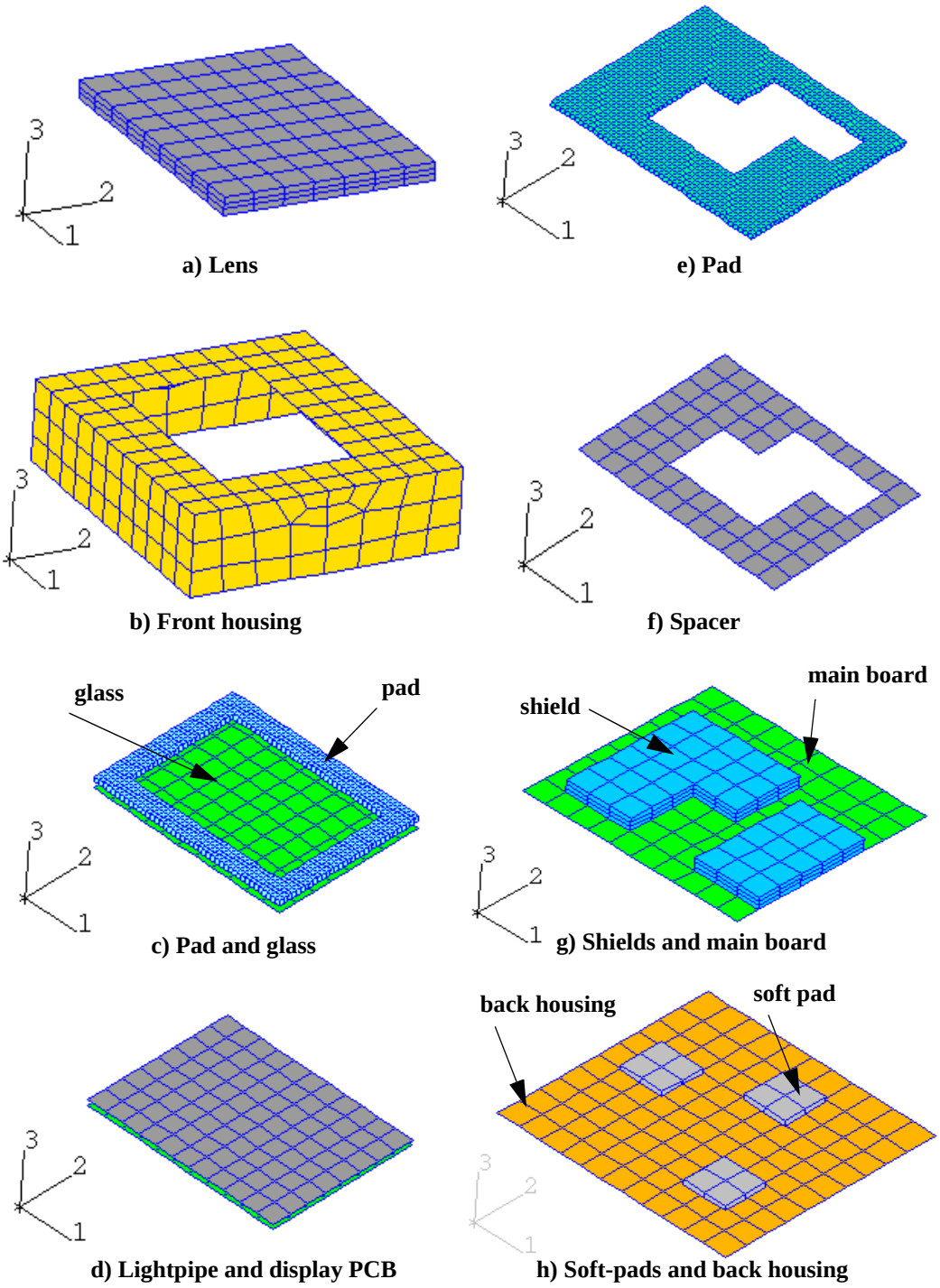

Figure 3: Components of coarse model for simplified two-way radio

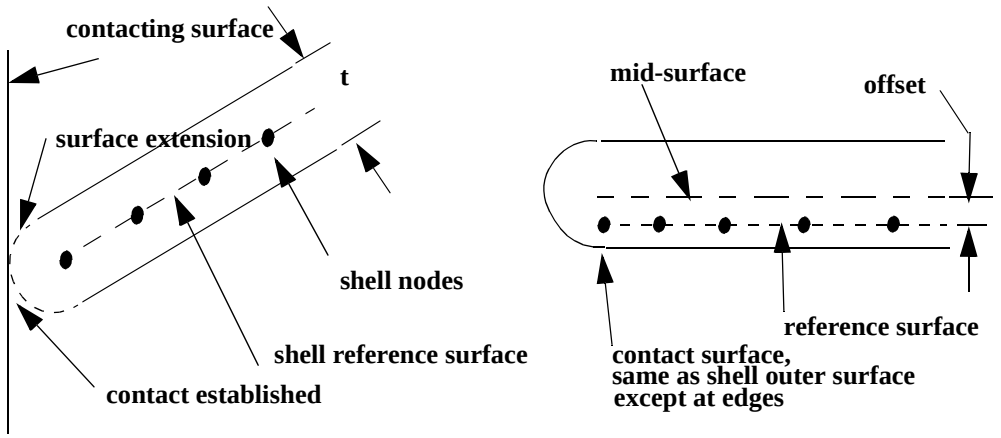

a) Edge contact **b) Shells with OFFSET option**

Figure 4: Bull-nose surface extension assumption utilized by ABAQUS' contact algorithm (pictures based on HKS documentation).

planes in the three-surface-stack to its true mid-surface location and not using the OFFSET option for that surface (or by modeling that component using solid elements).

The next difficulty in the analysis occurred with the elastomeric foam pads. These pads are very thin and extremely difficult to model. Their actual physical behavior under impact conditions is very nonlinear. Ideally, this would be modeled using a Gasket element. Unfortunately, Gasket elements only exist in /Standard, but not in /Explicit. As a result, a one-term *HYPERFOAM solid model was used here as an alternative. The analysis ran for about 1 msec of simulation time and then halted with the error message "The ratio of deformation speed to the wave speed exceeds 1.0 in at least one element". The error was caused by severe hourglassing in the solid elements of the elastomeric pads as they began to compress substantially (see Fig. 5). As is common with hourglassing problems, mesh refinement studies for the pads' solid elements were performed (in both the in-plane and the thickness directions). Several mesh refinements were tried, but none were able to take the solution significantly further. After additional study and discussions with HKS technical support, it was determined that the default hourglass control approach used in /Explicit is not well suited for modeling extremely thin *HYPERFOAM materials enduring such impact behavior. The final solution to this problem was to change the hourglass stiffness scaling factor from its default of 1.0 to a value of 50.0 (significantly outside the recommended range of 0.2 to 3.0). While this finally enabled the solution to run to completion, questions still remain as to the physical accuracy of this approach. Further research on modeling very thin elastomeric pads with explicit dynamics is needed.

Post processing the results in ABAQUS/Post indicated that some components had unintended rigid body motion. The cause of this motion was that /Explicit did not "tie" the parts together as

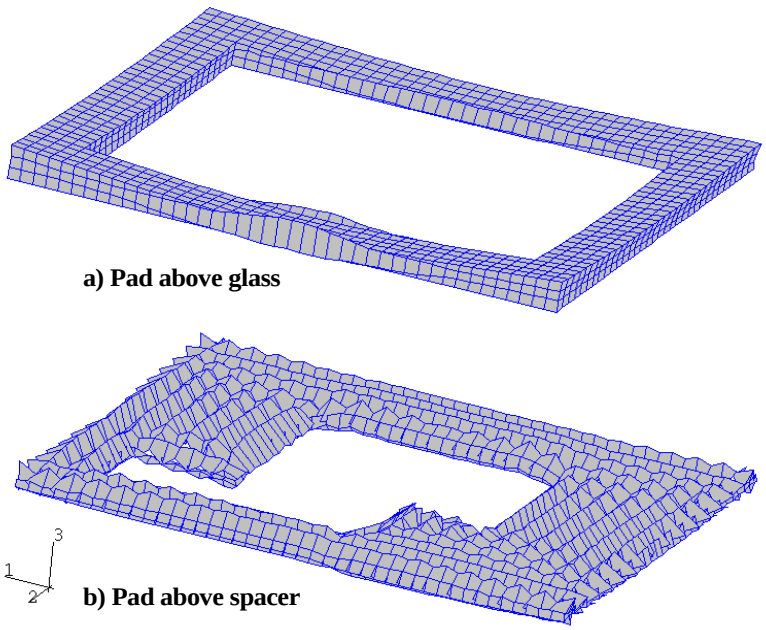

Note: The displacements are NOT magnified in these pictures (DMAG = 1.0)

Figure 5: Deformed shape of elastomeric pad elements when analysis halted.

was intended. This was corrected by using the ADJUST parameter on *CONTACT PAIR. Unfortunately, neither /Explicit nor /Post provides written or graphical information about nodes which are intended to be TIED (/Standard does provide this information in the dat file). Hopefully, this type of feedback will be provided graphically in future releases, preferably in the preprocessor (before the job is run).

The final debugged model in Figure 2 contained 18,000 DOF and took 1.75 CPU hours on an HP V-Class Unix compute server to analyze for 4 msec. This model had an average time increment of 0.163 μsec. To assess the influence of mesh refinement, a 50,000 DOF model (Fig.6) was analyzed. It had an average time increment of 0.0815 μsec and took 8.5 CPU hours. The vertical displacements of the ball, lens, and glass for the two models are shown in Figure 7 and appear fairly similar.

Whole-model energy plots for both meshes are shown in Figure 8. It is good practice to look at these types of energy plots to help validate an explicit dynamics model. A commonly quoted rule of thumb is that throughout the solution the ratio of artificial strain energy (ALLAE) to the physical internal strain energy should always be a small number (typically less than 5%). The physical internal strain energy is defined as all the other internal strain energies combined, namely: ALLSE + ALLPD + ALLCD + ALLQB + ALLEE (see ABAQUS/Explicit User's Manual). This energy check guideline historically comes from analyses such as car crash models that typically contain significant plasticity. The models being studied here are elastically-dominated impact problems, with negligible plasticity. Evaluating the coarse model (Fig. 8a), we see that this energy ratio is

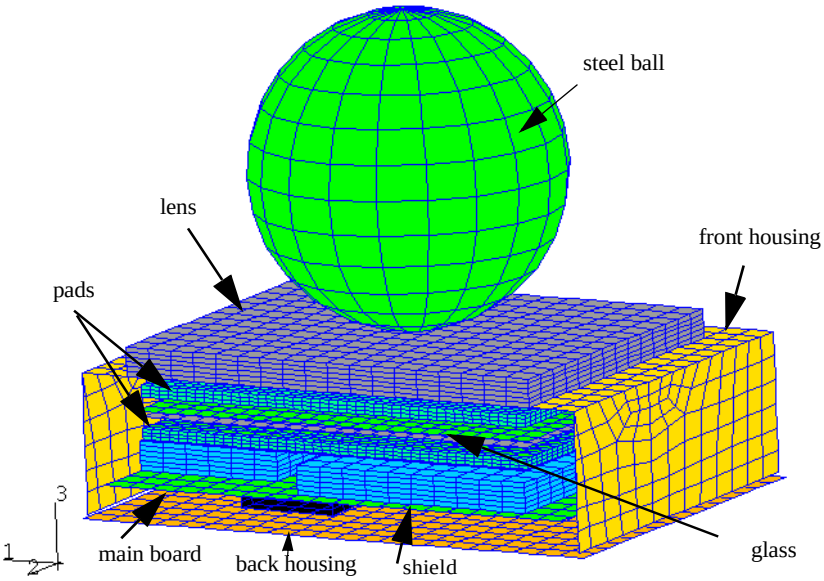

Figure 6: Refined finite element model of a simplified two-way radio

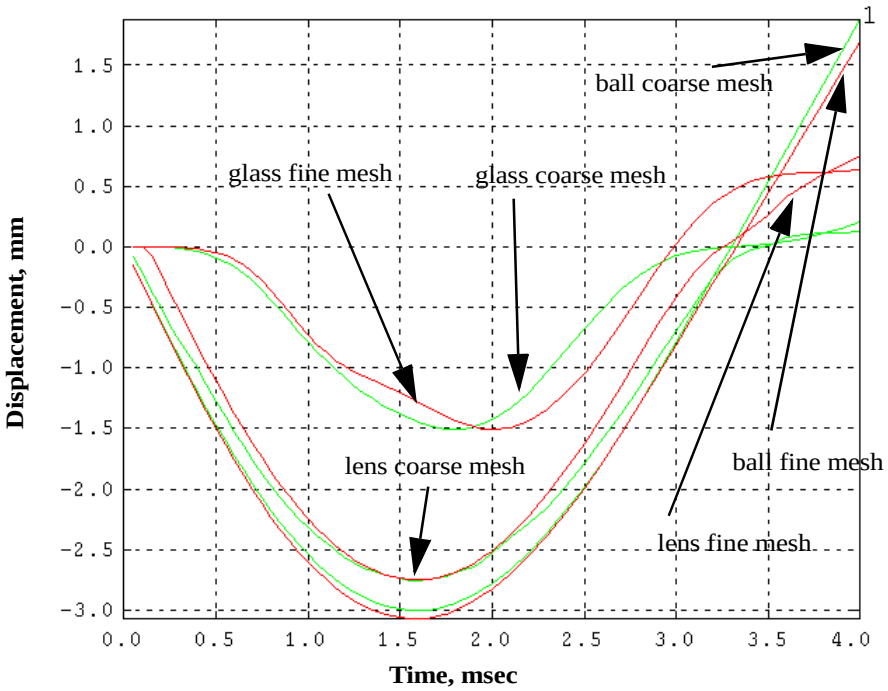

Figure 7: Vertical displacements under impact location for simplified models.

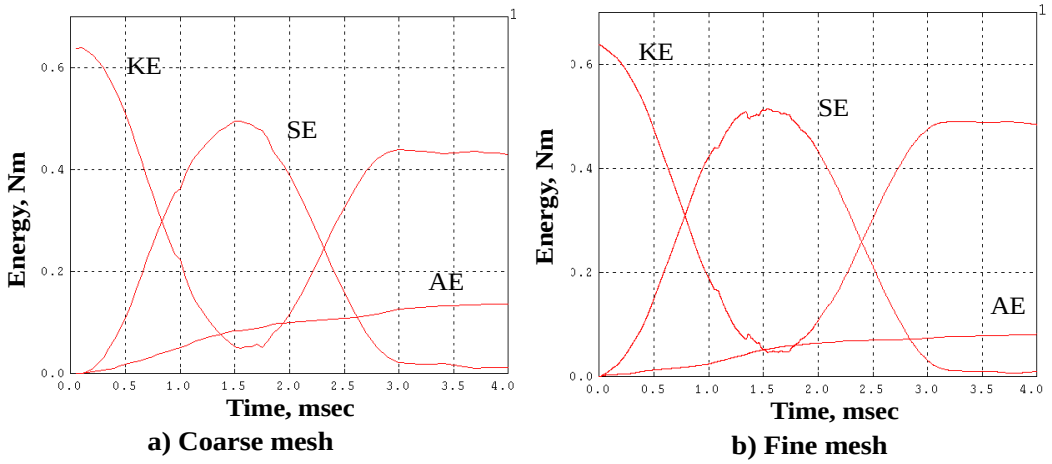

Note: KE - Kinetic Energy, SE - Recoverable (Elastic) Strain Energy, AE - "Artificial" Strain Energy

Figure 8: Whole-model energy plots for simplified radio models.

approximately 20% at 1.5 msec (maximum structural deformation) and approximately 800% at the end of the simulation! The refined model's ratios (Fig. 8b) are approximately 10% and 1000%, respectively. These results obviously do not satisfy the historic guidelines. It is important to understand that artificial strain energy is the energy associated with controlling the hourglass modes in reduced integration elements. It is composed of elastic and viscous mechanisms. A more appropriate energy check for an elastically-dominated impact problem is to compare this energy ratio at the peak value of the physical strain energy (typically just ALLSE). Based on this assessment, results still do not satisfy the 5% threshold, but they are close. Moreover, the results demonstrate that mesh refinement has helped. In our experience we find that artificial strain energy and hourglassing problems are not only caused by modeling thin elastomeric pads (as solids with *HYPERFOAM), but are also caused by shell elements (i.e. when a housing is impacted on its corner). This general topic needs further research and hopefully future element formulations can better handle these issues.

4.0 Detailed Model

We will now apply the previous lessons learned to a much larger, more detailed, representative model of the actual two-way radio originally shown in Figure 1. Details of the FE components used in this model are shown in Figures 9-11. The radio consists of 16 different parts which are grouped as 7 main components or sub assemblies. Components that were physically attached using adhesives were modeled using TIED contact. These included the lens to front housing, the glass to pad, the display PCB to pad, and the spacer to pad. Components that were simply stacked together physically were modeled using contact (without TIED option). For this study, the back housing was approximated with a simple rigid surface. All together, the model contained thirteen contact pairs.

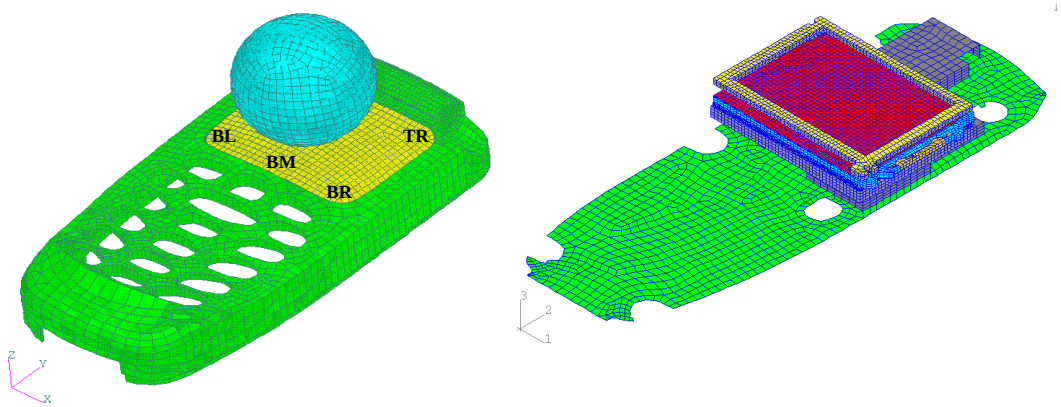

a) Lens, front housing and ball **b) Main board and display assembly**

Figure 9: Finite element model for detailed radio simulation

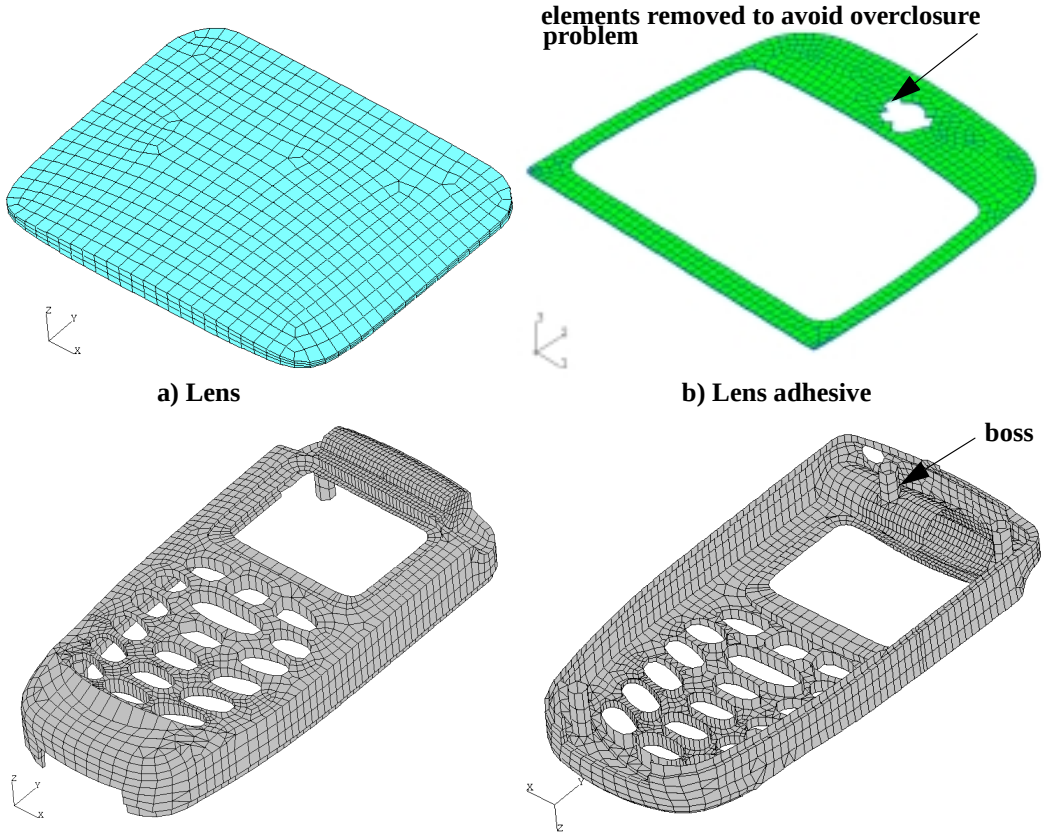

a) Lens **b) Lens adhesive**

c) Outside view **d) Inside view**

Figure 10: Meshed components for lens and front housing - detailed radio model.

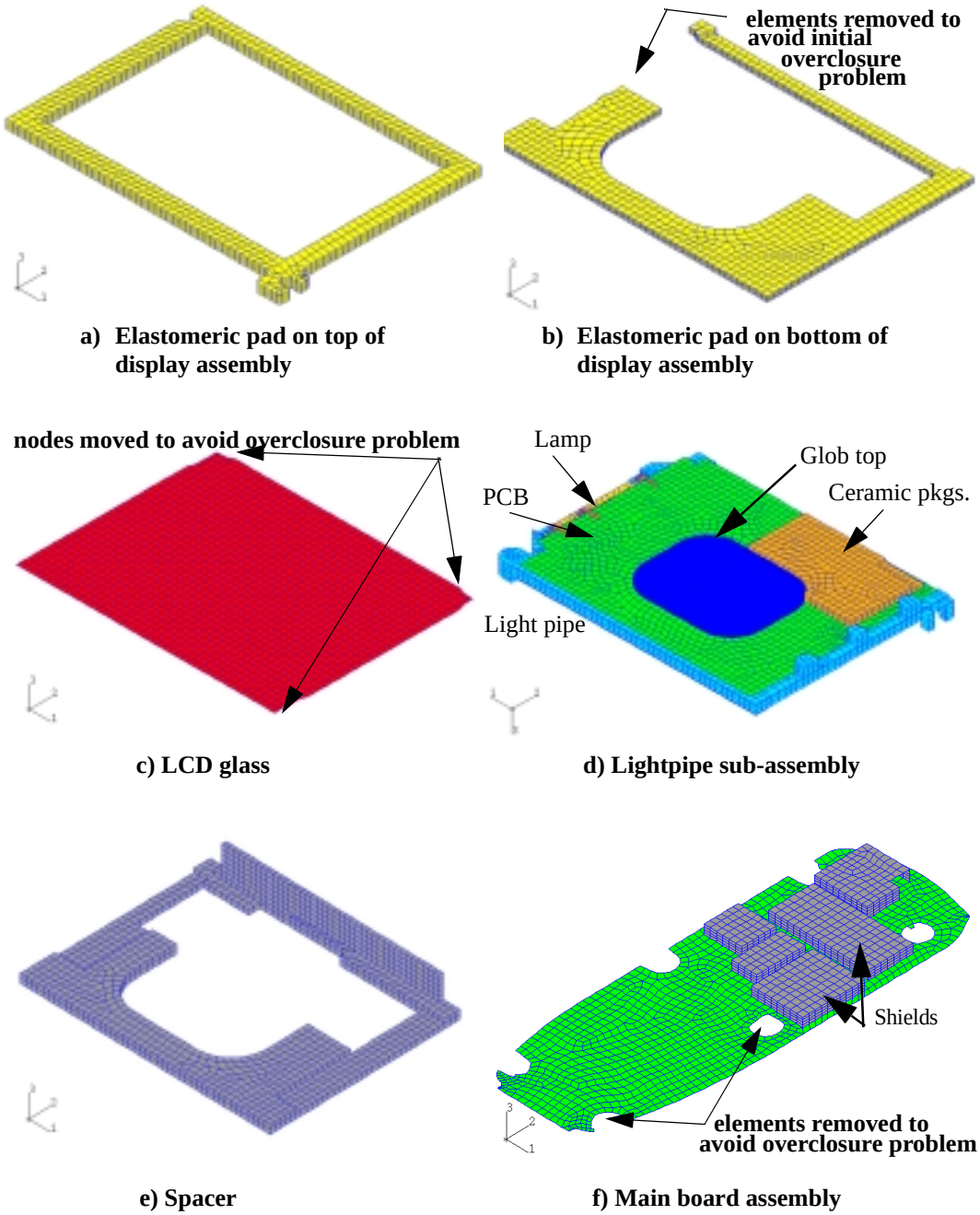

Figure 11: Meshed components for display assembly and main PCB - detailed radio model.

Building this model from the original Pro/E CAD database required using the combined approach outlined in Section 2.0. Especially troublesome in this particular model was the transformation and meshing of the “feature rich” front housing. Based on the lessons learned in Section 3.0, some slight modifications in modeling techniques were used here. The shields were modeled using shell (S4R) elements at their mid-plane (no OFFSET) since they were easily obtained from the CAD geometry. The lightpipe and spacer were modeled using solid (C3D8R) elements instead of shells to avoid overclosure problems associated with the multiple stacking of shells as well as to obtain more accurate contact behavior. The resulting model consisted of about 41,000 elements, 53,000 nodes and 200,000 DOF.

Debugging of the detailed model was dominated by problems with contact overclosures at several locations. The primary cause of most of the overclosures was the nonphysical bull-nose assumption used in the surface contact algorithms. These problems were more severe than in the simplified model because of the complexity of the geometry here. Overclosure issues were resolved by moving nodal coordinates in some cases (Fig. 11c) and by deleting elements in other cases (Fig. 10b & 11f). At one location, the overclosures were due to improper CAD geometry (between pad and the components on the display PCB). This issue was resolved by removing some of the pad elements at that location (see Fig. 11b). A rather difficult overclosure error to debug occurred between the shell elements in the front housing and solid elements of the pad (above the glass). Based on numerous checks, it appeared that the two surfaces were not overclosed, yet the code continued to complain. The final solution to the problem was to switch the MASTER and SLAVE default definitions by using the WEIGHT option in the contact pair definition.

Initial analyses of the model required an average time increment of 16.4 nano-second, ten times smaller than the coarse mesh from the simplified model. Further evaluation of the detailed model indicated that this time increment was controlled by a few small elements in the lightpipe assembly which were far away from the point of interest. Remeshing in this particular area to increase the size of these small elements would be extremely time consuming. Instead, we utilized ABAQUS’s automatic mass scaling feature (*FIXED MASS SCALING) to mass scale these elements by a factor of 10. This created an increase in the time increment to 30.6 nano-second, resulting in a 45% decrease in total solution time!

During the initial runs of this model, wave speed problems caused the solutions to prematurely halt before 1.0 msec of simulation time. The error message “The ratio of deformation speed to the wave speed exceeds 1.0 in at least one element” was being caused by solid elements in the elastomeric pad that were located between the glass and the front housing (see Fig. 9, location denoted as BM). This problem was occurring despite the fact we were using the very aggressive hourglass stiffness scaling factor of 50 (determined from Section 3.0). Both hourglass control and mesh refinement was varied in an attempt to overcome the problem. Only refining the elastomeric pad mesh to four elements through its thickness created any improvement (one through six layers were tested). This allowed the model to run for 1.3 msec before halting.

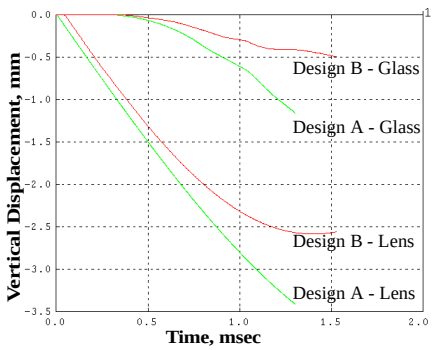

a) Centerpoint vertical displacement

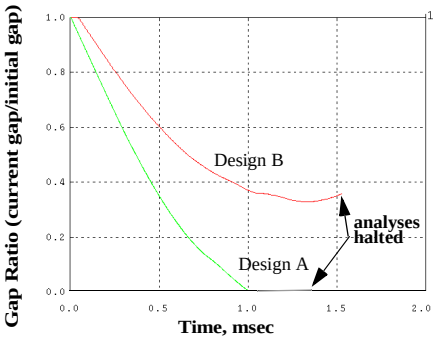

b) Gap ratio at centerpoint

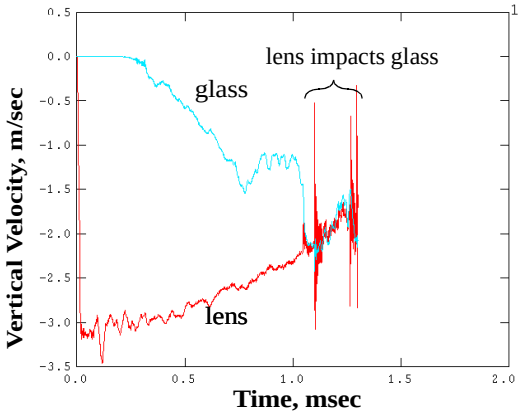

c) Centerpoint vertical velocities - Design A

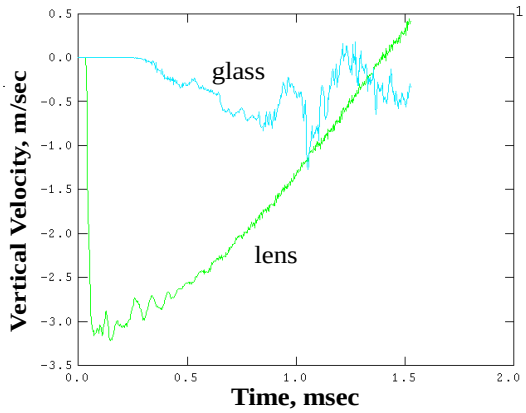

d) Centerpoint vertical velocities - Design B

Figure 12: Displacement and velocity results for designs A and B for detailed radio model.

To follow the design that was evolving at the time of this analysis, the original detailed model (called Design A) was slightly modified by changing a few geometric parameters, resulting in a stiffer lens and housing (denoted as Design B). The discussions that follow show typical analysis results that can be obtained in a design study for these types of impact problems.

4.1 Analysis and Results

Figure 12 displays the vertical motion of the display lens and LCD glass for both designs due to a ball dropping onto the center of the lens. Also displayed in the figure is the gap ratio for both designs. This is defined as the gap between lens and glass, normalized with respect to the initial gap. It was desired that both models simulate for 3 msec of time. Unfortunately, both simulations

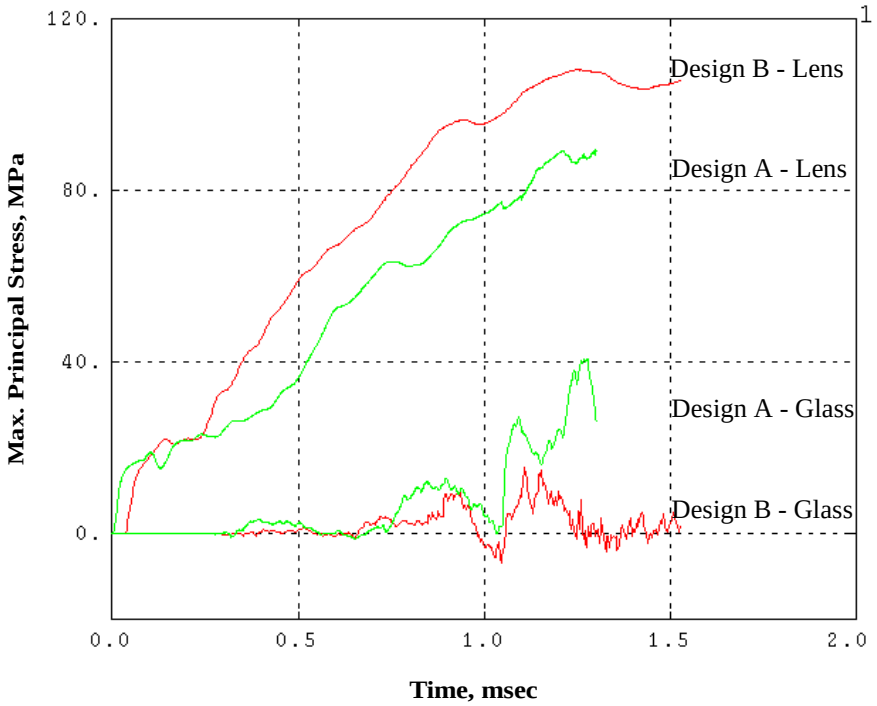

Figure 13: Maximum principal stress under the point of impact - detailed model.

halted prematurely due to wave speed problems with the elastomeric pads. Design A ran for 1.30 msec and Design B ran for 1.52 msec (requiring 26 CPU hours). Despite the fact that the simulations did not run for the entire time desired, several important design assessments could be made. Figure 12b clearly shows that the lens hit the glass LCD in Design A (gap ratio became zero) and that it does not for Design B. The vertical velocity plots of Figure 12d confirm the conclusion that the primary deformation due to the impact has occurred in Design B (lens velocity has become positive). Figure 12c also demonstrates how variables such as velocity can become extremely noisy when impacts occur. To avoid any aliasing errors, the velocity plots were plotted using every solution increment (see Diehl, 1999, for a detailed discussion of this topic). Figure 13 depicts the stress in the lens and glass, again plotted at every increment to avoid aliasing errors.

The whole-model energy plots of Figure 14 show that the ratio of artificial strain energy to elastic strain energy for the analyses at the peak value of elastic strain energy is less than 5%, passing the guideline for this type of check. The low values of this ratio are attributed to the fact that the mesh density in these detailed models is much greater than that used in the preliminary analysis of Section 3.0. Its interesting to note that even though the detailed models passed this energy ratio check, their solutions prematurely halted because of wave speed problems caused by

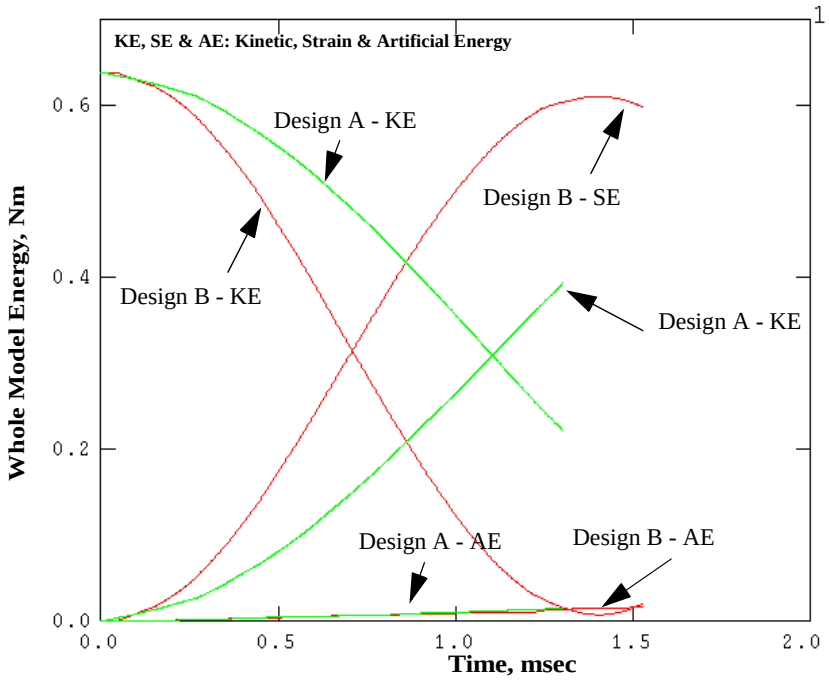

Figure 14: Whole-model energies for design A and B - detailed models.

hourglassing. This further implies that additional research is needed to better understand these issues, especially for elastically-dominated impact problems.

Figure 15 shows vertical displacements for Design B when the ball was dropped at the upper corner of the lens instead of the center of the lens. For this impact location, the model was able to run for the entire 3.0 msec of intended simulation time (requiring 57 CPU hours). Remember, the only difference in this case is impact location! We believe that the success of this analysis was due to the presence of a boss near that corner of the lens (shown in Fig. 10d) which locally stiffened the housing in that area. This increased support sufficiently decreased the deformation of the elastomeric pads such that severe hourglassing and wave speed problems were avoided. This result has some interesting implications. It demonstrates that the modeling approach used for the elastomeric pads can be successful, provided that the impact loading is not extreme. Secondly, it demonstrates an uncertainty level that can exist in these types of elastically-dominated impact problems. A model might run fine for certain loading scenarios, but given a particular loading case (which is not known ahead of time), it might have significant trouble running to completion.

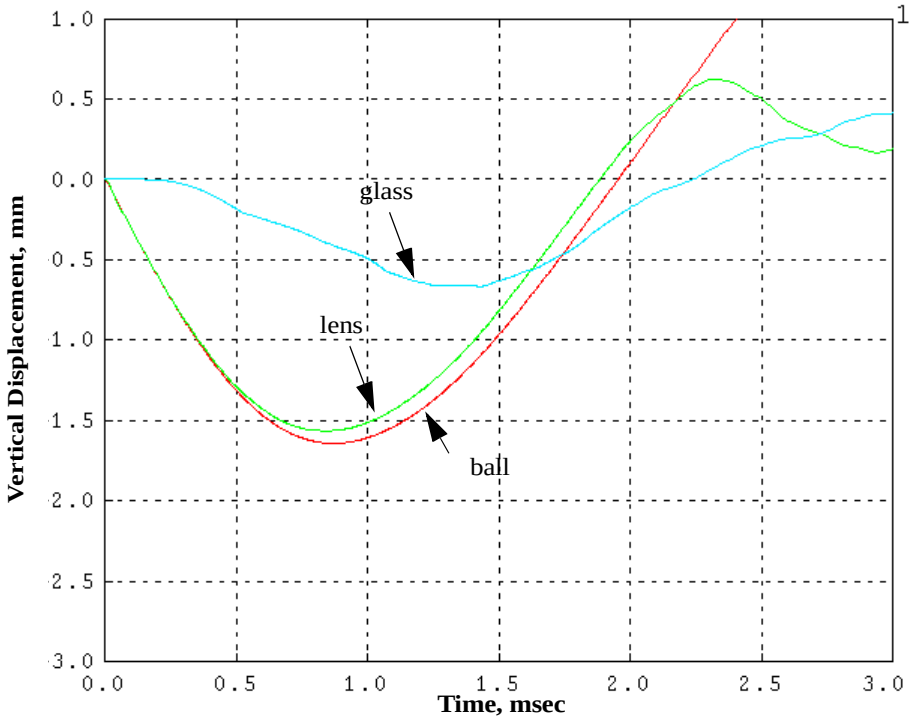

Figure 15: Results when ball was dropped on corner of lens - design B.

5.0 Conclusions

Explicit dynamic simulations are very useful to analyze structures enduring drop and impact loading. This study has focused on utilizing ABAQUS/Explicit to analyze the very challenging class of elastically-dominated impact problems that are common in consumer electronic devices. From the present study of a ball drop simulation for a two-way radio, the following conclusions are drawn:

1. Analysis of impact and drop loading for real-world two-way radio product designs can be achieved with ABAQUS/Explicit. The ability to utilize ABAQUS' extensive contact capabilities is key to creating physically representative models.

2. Transformation of the designer's CAD geometry into usable FE models still consumes large portions of time. Continued and aggressive development in this area is required.

3. TIED contact, along with the ADJUST parameter, is extremely useful for connecting two components with dissimilar meshes. This can save significant meshing time. HKS needs to enable graphical feedback (in the preprocessing stage) of which nodes are actually "TIED" by the code.

4. The OFFSET option for shells is extremely useful, removing the requirement to obtain mid-plane meshes. In cases where a stack of three or more shells are interacting with each other via contact, models containing initial overclosures for these elements should be avoided.

5. Selective mass scaling via the *FIXED MASS SCALING feature is easy to use and can significantly improve solution times while retaining solution accuracy.

6. HKS's contact algorithms utilize a non-physical "bull-nose" surface extension assumption for all contact surfaces. This artificially extends the free edges of contact surfaces beyond their actual location, causing numerous and severe overclosure errors in complex models. HKS needs to provide alternative choices to their bull-nose approach. Additionally, they need to provide tools to visualize the actual thickness of these surfaces, not only for model debugging, but also to aid in the evaluation of structural motion as the solution develops (i.e. "Are two surfaces contacting each other?").

7. HKS or the FE preprocessor community needs to provide a complete method to map the continual thickness variations of sculpted CAD solid geometry onto shell models. ABAQUS currently offers a feature to include a nodal table of such data, but no tools exist to produce this data.

8. Modeling very thin elastomeric foamed pads under impact conditions is extremely difficult. They are highly prone to problems with wave speed errors caused by hourglassing. A partial solution to these problems was obtained by applying extremely aggressive values of hourglass control parameters, far outside the range of suggested values. Further research into actual material behavior, constitutive models, and element formulations is required. Application of a Gasket model in ABAQUS/Explicit similar to that available in ABAQUS/Standard might be a better solution.

9. Artificial strain energy ratio checks for elastically-dominated impact problems should be assessed at the peak value of the physical internal strain energy (typically ALLSE). To minimize artificial strain energy growth, relatively refined element meshes are required.

References

ABAQUS/Explicit User's Manual, Version 5.7.

Diehl, T., Carroll, D., and Nagaraj, B. K., "Using Digital Signal Processing (DSP) to Significantly Improve the Interpretation of ABAQUS/Explicit Results," *ABAQUS Users Conference Proceedings*, May 25-28, 1999.